JOURNAL OF SOLID STATE CHEMISTRY 3, 387–400 (1971)

Self-Diffusion and the Defect Structure of Cadmium Sulfide*

V. KUMAR† AND F. A. KRÖGER

Department of Materials Science, University of Southern California, University Park, Los Angeles, California 90007

Received January 4, 1971

Cd and S tracer diffusivities were measured in undoped and In-doped CdS crystals as a function of temperature, the partial pressure of Cd or S_2, and In concentration. Above 700°C and under high Cd pressures, sulfur diffuses by a vacancy mechanism involving the doubly ionized vacancy $V_S^{\cdot\cdot}$; this vacancy is also the major electrically active point defect and is the commonly reported double donor in CdS. Under these conditions, Cd diffusion occurs by singly ionized Cd interstitials, these interstitials being the fastest moving point defects, but only a minority as donors compared to S vacancies. Under high S_2 pressures, sulfur diffuses by the interstitial mechanism involving the neutral $S_i^{\times}$ interstitials. Cd diffusion under these conditions is controlled by doubly ionized Cd vacancies. Experiments on indium-doped samples show that at moderate-to-high Cd pressures In is incorporated with the release of an equal number of electrons into the conduction band, whereas at low Cd pressures, the incorporation occurs with the creation of doubly ionized native acceptors. These acceptors are most probably the Cd vacancies responsible for Cd diffusion in this range of Cd pressures.

The absolute mobilities of $V_S^{\cdot\cdot}$, V_{Cd}'' and $(In_{Cd}\,V_{Cd})'$ have been determined, assuming $[V_{Cd}''] > [S_i'']$. For $Cd_i^{\cdot}$ and $S_i^{\times}$ a separation of diffusivities into mobilities and concentrations was not possible. Estimates for the position of the acceptor levels of V_{Cd} are obtained.

Introduction

A large amount of work has been done on the physical properties of CdS. Although it has been recognized for a long time that these properties are largely determined by various defects present, much less effort has gone into the identification of the relevant defects and the dependence of their concentrations on the conditions of preparation of the crystals. Following the approach of Kröger and Vink (*1*), it is possible to develop models (defect structures) that can successfully explain all the observed properties and their variation with the conditions of preparation.

This approach was in fact first applied to CdS by Kröger et al. (*2*) to explain the results of Hall-effect, conductivity and optical absorption measurements done on undoped and donor (Ga, Cl) doped crystals after the crystals had been quenched after equilibration in an environment with well-defined Cd pressure and temperature. Although the conclusions reached were not entirely correct in the light of the information that has since become available, the basic approach is still valid.

Boyn et al. (*3*, *4*) performed conductivity experiments on CdS between 400°C and 730°C under well-defined Cd and S atmospheres. They concluded that under Cd atmospheres the conductivity is controlled by a doubly ionizable donor, Cd_i. At temperatures above 540°C, $Cd_i^{\cdot\cdot}$ are the dominant point defects, leading to an electronic conductivity $\sigma \propto p_{Cd}^{1/3}$. Below this temperature, predominance of Frenkel disorder ($[Cd_i^{\cdot\cdot}] \approx [V_{Cd}'']$) was proposed as the explanation of the observed dependence $\sigma \propto p_{Cd}^{1/2}$, the ionized donor still being $Cd_i^{\cdot\cdot}$. Frenkel disorder was considered dominant under S atmospheres at high as well as low temperatures. A double donor has also been reported for CdSe (*5*, *6*, *34*). For CdTe in Cd vapor at high temperatures, some authors report a doubly ionized donor (*7*, *8*, *9*), others report a singly ionized donor (*10*). Recently, the presence of a double donor in CdS has been confirmed by Hershman and Kröger (*11*).

Recognizing the existence of a relation between

* This work was supported by the National Science Foundation under Grant GK-4056.

† Now at Bell Telephone Research Laboratories, Murray Hill, New Jersey.

ion transport, deviations from stoichiometry and the defect structure of a compound as stated by Wagner (*12*), Seltzer et al. (*13*, *14*) studied the defect structure of PbS through Pb and S tracer diffusion. A reasonably complete picture of the transport properties and the relevant defects was thus obtained. Similar work has been attempted for Cd and Zn chalcogenides.

Chalcogen tracer diffusion results of Woodbury and Hall (*15*) on Se and Te in various Cd and Zn chalcogenides, and of Borsenberger et al. (*16*) on Te in CdTe, show that in all cases the neutral chalcogen interstitial is the controlling chalcogen species for diffusion under high chalcogen pressures. At high Cd pressures, dominance of a different species is indicated. The situation for the metal component tracer diffusion is more diverse. Woodbury (*17*) and Whelan et al. (*18*) found that in CdS, Cd tracer diffusion under high Cd pressures is controlled by neutral Cd interstitials, whereas under high S_2 pressures the doubly ionized vacancy, V''_{Cd}, is the controlling species for Cd diffusion. Whelan and Shaw concluded to the presence of neutral interstitials from the dependence $D^*_{Cd} \propto p_{Cd}$ under high p_{Cd} at 850°C. Borsenberger et al. (*17*) found a pressure dependence of the form $D^*_{Cd} \propto p_{Cd}^{1/2}$ for CdSe under these conditions and ascribed it to the singly ionized Cd interstitial, $Cd_i^{\cdot}$, controlling the charge neutrality as well as Cd diffusion, the counterpart defect for charge neutrality being electrons. This contradicts the dependence $[e'] \propto p_{Cd}^{1/2}$ found by other authors under similar conditions (*5*, *6*). Borsenberger et al. (*16*) and Whelan et al. (*20*) found D^*_{Cd} in CdTe to be independent of p_{Cd} over the entire range of stability. The former ascribed it to a dominant Frenkel disorder involving Cd interstitials and vacancies. The observation that Cd diffusion was enhanced by donor as well as acceptor impurities led them to the conclusion that the defects could not be associated Frenkel pairs, but must be separate species controlling charge neutrality. This, however, contradicts the observation $[e'] \propto p_{Cd}^{1/3}$ of other authors (*7*, *8*), unless the Cd interstitials are assumed to be triply ionized and compensated for charge neutrality by triply ionized Cd vacancies, a very unlikely situation. Neutral associated Frenkel pairs, on the other hand, do not transport Cd and, therefore, cannot explain the p_{Cd} independence of the chemical diffusivity reported by Zanio (*9*).

Clearly, the defect structure of these materials is not yet understood. In the present paper, we report the results of a study of the self-diffusion of Cd and S in CdS as a function of p_{Cd}, T, and impurity concentration. As we shall see, combination with the Hall-effect data referred to earlier (*11*), leads to an almost complete clarification of the defect structure and the thermodynamic parameters of defect formation.

Theoretical

1. Tracer Diffusion and Defect-Chemistry

Tracer self-diffusion is the gradual replacement of the nontracer atoms of an element in the crystal by tracers of the same element, starting from a source and proceeding towards regions in the crystal away from this source. Microscopically, it results from the jump processes involving point defects in the crystal and can be described macroscopically by Fick's equations (unidimensional) for the particle current J and the variation of the concentration:

$$J = -D^* \frac{dc}{dx} \tag{1}$$

and

$$\frac{dc}{dt} = D^* \frac{d^2 c}{dx^2}, \tag{2}$$

where (2) follows from (1), using mass balance and assuming D^* to be independent of concentration, a condition obviously satisfied by tracers.

D^*, which is the measured quantity for diffusion experiments, is determined by the dominant diffusion mechanism (*12*). Cadmium and sulfur vacancies and interstitials or associates of these species are the only defects important for tracer transport. If we concentrate on the single defects, we may have cadmium vacancies (V_{Cd}) and interstitials (Cd_i) causing Cd exchanges, and V_S and S_i causing sulfur exchange. Each mechanism is further differentiated according to the charge state of the defect. In other words, $Cd_i^{\times}$, $Cd_i^{\cdot}$, and $Cd_i^{\cdot\cdot}$ lead to separate tracer fluxes. For each species, the flux depends on the product of the microscope diffusivity of the defect, D_j, and the concentration of the defect expressed as a site fraction, $[j]$. Summing over the various defects involved,

$$D_j^* = \sum D_j[j]. \tag{3}$$

The justification of this relation is different for interstitial diffusion and vacancy diffusion. In the former case, it is due to the fact that although diffusion takes place via the interlattice, the tracers are distributed between normal lattice sites and interstitial sites in the same way as the normal atoms are. If this distribution equilibrium is not maintained during the diffusion, (3) would not hold. Now $D_j^* = D_j$. For the vacancy diffusion mechanism, (3) results from the fact that tracer jumps are possible

only if a vacancy is present at a neighboring site. Therefore, for this mechanism, (3) is always valid. D_j depends on temperature according to

$$D_j = D_j^0 \exp(-\Delta H/kT),$$

ΔH being the free enthalpy of activation of the tracer jump to the next site. $[j]$ depends on the composition of the crystal, the component activities, the pressure, and the temperature.

If we carry out diffusion studies at constant temperature, D_j = constant, and thus variations in D_j^* are due to variations in $[j]$. The way in which $[j]$ depends on the composition and the conditions of preparation is described satisfactorily by imperfection chemistry (1). Table I lists several defect formation reactions for CdS, and the corresponding mass action relations. Reactions (a)–(i) are involved in establishing deviations from stoichiometry. Reactions (j), (k), and (l) create atomic and electronic disorder. In crystals doped with the foreign donor indium, defects $In_{Cd}^{\cdot}$ and associates such as $(In_{Cd}\,V_{Cd})'$ formed by reaction (q) have also to be taken into account. Since the In_{Cd} donor level is close to the conduction band, ionization is always complete, i.e., $In_{Cd}^{\times}$ does not occur in appreciable concentrations.

Pairs between foreign donors and vacancies have been shown to be the activator centers of the so-called self-activated luminescence in ZnS [*21*, *22*], and there is little doubt that such associates will also occur in CdS. The formation at high temperatures has been discussed by Prener and Weil (*23*). It remains an open question, however, whether the pairs are formed by equilibration at high temperature, or that they are formed during cooling (*24*). This is one of the points we shall pay attention to in the present study.

The mass action relations given in Table I are given in terms of concentrations. For the atomic defects, this is justified as long as the concentrations are smaller than, say, 1 %. For electrons, $[e']$ has to be replaced by $a_e = \gamma[e']$ with γ, the activity coefficient, being >1 in degenerate samples.

Concentrations of defects as $f(p_{Cd}, T, [In]_{total})$ can be found by solving the simultaneous equations (a)–(q) complemented by the neutrality condition (r) and the indium balance (s) (*1*). Following Brouwer (*25*), approximate solutions can be obtained by using only the dominant terms in (r) and (s). The solutions valid in a certain range are of the general form $[j] = \prod_s K_s p_{Cd}^n [In]_{total}^m$, with n and m simple fractions or small numbers. Figure 1 shows defect isotherms for CdS doped with a foreign donor D arrived at in this manner; pairing is neglected. This figure demonstrates the complications to be expected even in this simplified case. A similar result,

TABLE I

DEFECT FORMATION REACTIONS FOR CdS AND THE CORRESPONDING MASS ACTION RELATIONS

Reaction		Mass action relation	
$Cd(g) \rightleftarrows Cd_{Cd}^{\times} + V_S^{\cdot\cdot} + 2e'$	; H_{SV}''	$K_{SV}'' = [V_S^{\cdot\cdot}][e']^2/p_{Cd}$	(a)
$V_S^{\times} \rightleftarrows V_S^{\cdot} + e'$	; E_{d_1}	$K_{d_1} = [V_S^{\cdot}][e']/[V_S^{\times}]$	(b)
$V_S^{\cdot} \rightleftarrows V_S^{\cdot\cdot} + e'$	; E_{d_2}	$K_{d_2} = [V_S^{\cdot\cdot}][e']/[V_S^{\cdot}]$	(c)
$Cd(g) \rightleftarrows Cd_{Cd}^{\times} + V_S^{\times}$	; H_{SV}	$K_{SV} = [V_S^{\times}]/p_{Cd}$	(d)
$Cd_{Cd}^{\times} + 2e' \rightleftarrows Cd(g) + V_{Cd}''$	; H_{CdV}''	$K_{CdV}'' = [V_{Cd}''] p_{Cd}/[e']^2$	(e)
$V_{Cd}'' \rightleftarrows V_{Cd}^{\times} + 2e'$	; $E_{V_1} + E_{V_2}$	$K_{V_1} K_{V_2} = [e']^2 [V_{Cd}^{\times}]/[V_{Cd}'']$	(f)
$Cd_{Cd}^{\times} \rightleftarrows Cd(g) + V_S^{\times}$	; H_{CdV}	$K_{CdV} = [V_{Cd}^{\times}] p_{Cd}$	(g)
$S_S^{\times} \rightleftarrows S(g) + V_S^{\times}$	; H_{SVG}	$K_{SVG} = [V_S^{\times}] p_S$	(h)
$Cd(g) + V_i^{\times} \rightarrow Cd_i^{\cdot} + e'$	; H_{Cd_i}	$K_{Cd_i} = [Cd_i^{\cdot}][e']/p_{Cd}$	(i)
$0 \rightleftarrows e' + h^{\cdot}$	; E_I	$K_I = [e'][h^{\cdot}]$	(j)
$0 \rightleftarrows V_{Cd}'' + V_S^{\cdot\cdot}$	; H_S''	$K_S'' = [V_{Cd}''][V_S^{\cdot\cdot}]$	(k)
$0 \rightleftarrows V_{Cd}^{\times} + V_S^{\times}$	; H_S	$K_S = [V_{Cd}^{\times}][V_S^{\times}]$	(l)
$CdS(s) \rightleftarrows Cd(g) + \frac{1}{2}S_2(g)$	; H_{CdS}	$K_{CdS} = P_{Cd} p_{S_2}^{1/2}$	(m)
$CdS(s) \rightleftarrows Cd(g) + S(g)$	; $H_{Cd,S}$	$K_{Cd,S} = p_{Cd} p_S$	(n)
$S_2(g) \rightleftarrows 2S(g)$	; H_D	$K_D = p_S^2/p_{S_2}$	(o)
$Cd(l) \rightleftarrows Cd(g)$	; H_{Cd}	$K_{Cd} = p_{Cd}\, a_{Cd(l)}$	(p)
$In_{Cd}^{\cdot} + V_{Cd}'' \rightleftarrows (In_{Cd}\,V_{Cd})'$	; H_P	$K_P = [(In_{Cd}\,V_{Cd})'']/[In_{Cd}^{\cdot}][V_{Cd}'']$	(q)

Neutrality Condition: $[e'] + [V_{Cd}'] + 2[V_{Cd}''] + [S_i'] + 2[S_i''] + [(In_{Cd}\,V_{Cd})'] = [h^{\cdot}] + [Cd_i^{\cdot}] + 2[Cd_i^{\cdot\cdot}] + [V_S^{\cdot}] + 2[V_S^{\cdot\cdot}] + [In_{Cd}^{\cdot}]$ (r). Indium Balance: $[In_{Cd}^{\cdot}] + [(In_{Cd}\,V_{Cd})'] \simeq [In]_{total}$ (s).

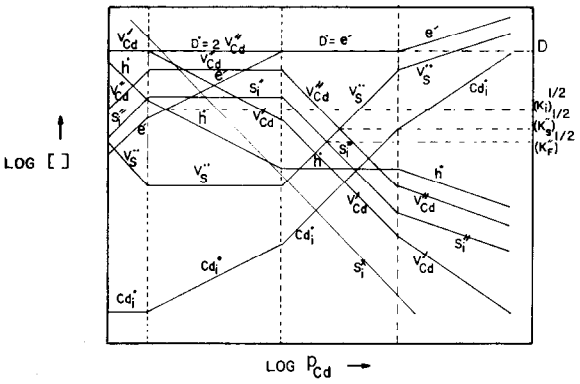

FIG. 1. Defect isotherms for donor-doped CdS calculated with the assumption that V''_{Cd} is the major doubly ionized native acceptor whereas pairing is neglected.

with pairs taking the place of V''_{Cd}, is obtained for the case that pairs are dominant (*24*).

2. Solution of the Diffusion Equation

For a semiinfinite medium and a constant activity tracer source, the solution of the one-dimensional diffusion equation (2) is (*26*):

$$c(x,t) = c_0 \operatorname{erfc}\left(\frac{x^2}{4Dt}\right)^{1/2}. \qquad (4)$$

Steps were taken to assure that the above conditions are satisfied in the experiments to be described. Here tracer diffuses from the vapor into a relatively thick crystal while a constant activity or partial pressure of the component loaded with the tracer is maintained around it. For a 1 mm thick plate-shaped crystal, with diffusion proceeding from both sides, a tracer penetration of 100μ from each side is within the realm of a semiinfinite medium. For a fixed Dt product, (4) defines a unique $c - x$ profile starting at c_0. A log $c - x^2$ plot is for the most part a straight line (see Fig. 3).

Experimental

1. Specimen Preparation

Unoriented CdS single crystals were received as $1 \times 1 \times 1$ cm^3 pieces from the Clevite Corporation, Cleveland, Ohio. Mass spectrographic analyses for these crystals are shown in Table II. Plates $5 \times 5 \times 1$ mm^3 in size and parallel to one of the faces of the received crystal were cut from these. The plates were polished and etched with 50% HCl to give a smooth flat surface finish. These were rinsed and then cleaned in boiling deionized water.

TABLE II

CdS MASS SPECTROGRAPHIC ANALYSIS

(Concentrations in Parts per Million Atomic)

Element	Detection limit	Clevite I	Clevite II	Clevite III
H	0.2	12	5.4	0.52
Li	0.003	0.005	N.D.[a]	0.005
C	0.01	7.5	1.2	1.3
N	0.01	0.12	0.074	0.063
F	0.03	N.D.[a]	N.D.[a]	N.D.[a]
Na	0.003	0.035	0.030	0.061
Si	0.1	N.D.[a]	N.D.[a]	N.D.[a]
Cl	0.03	0.05	0.05	0.10
K	0.003	0.0098	0.004	0.0062
Ca	0.007	0.22	0.031	0.01

[a] Note: N.D. = Not detected. Other impurities not listed were not detected and have concentrations less than 0.1 ppma, except Mn, Fe, O, and Zn, which are interfered with by background lines of sulfur and cadmium.

Indium-doped samples were prepared in batches of four to ensure uniform doping in a group of experimental specimens. A known amount of In was either deposited as a thin film by evaporation and converted to In_2S_3 by passing H_2S over the samples, or a piece of indium metal was sandwiched between two CdS plates ($5 \times 10 \times 1$ mm^3). The crystal plates or the sandwiches containing In in one form or the other were then fired in thick wall (2 mm) quartz ampoules with addition of enough sulfur to give sulfur vapor at a pressure of 8–10 atmospheres at 950°C. The firing was carried out for 7–10 days. After cooling at the end of this period, the initially yellow CdS crystals have become red in color. The red color is deeper, the higher the In concentration. This provides a rough check on relative In concentration in various samples.

The crystals were polished, etched with HCl and rinsed in deionized water. The homogeneity of doping was checked with the aid of an electron microprobe at various points on the crystal. The exact donor concentration was determined by measuring the room temperature electron concentration in one of the samples after it had been fired for a day at about 800°C under Cd vapor (~1.5 atmosphere). This was accomplished through the Hall effect using Van der Pauw's method (*27*). Donor concentrations up to ~10^{20}/cm^3 were measured in this manner. The measured concentrations were within 20% of those determined from the amount of dopant used.

2. Tracer Diffusion

Cadmium tracer (^{109}Cd, γ, 0.09 MeV, 1.3 years) was received from New England Nuclear Corp. as $CdCl_2$ in 0.5N HCl in batches of 1 mCi. After dilution, a few drops of the solution containing about one μCi of activity were chemically converted to traces of CdS inside small quartz tubes (3 mm i.d., 2 cm long). For use of Cd* in diffusion runs under Cd vapor, the tracer in the small tube was leached out into small beads of Cd metal by heating the tube along with 25–30 mg of Cd in vacuum sealed quartz ampoules at 900°C followed by slow cooling. For use of Cd* in experiments under sulfur vapor, the tubes with traces of Cd*S were used as such. Sulfur tracer (^{35}S, β, 0.168 MeV, 89 days) was received as a solution of elemental sulfur in benzene. Wherever needed, a few drops of this solution were allowed to evaporate inside the tube or ampoule leaving behind elemental sulfur containing the tracer.

In order to carry out a tracer diffusion experiment under well-defined conditions, the temperature of the crystal and the p_{Cd} or p_{S_2} around it have to remain constant throughout the experiment. To satisfy the boundary conditions for solution (4), a constant source of tracer either in the vapor or on the surface has also to be provided. Diffusion specimens being small, a constant temperature was easily maintained with the help of a controlled furnace. The other two conditions, which are linked together if the tracer source is in the vapor, are a little more difficult to satisfy.

For a given crystal temperature, the range of p_{Cd} or p_{S_2} with which the crystal can be in equilibrium is limited (see Fig. 2). The high and low p_{Cd} limits

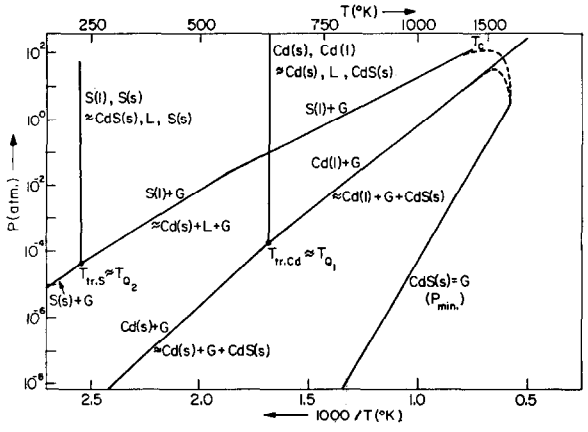

FIG. 2. P–T projection for the system Cd–S, with P_{min} according to Ref. (28).

are determined largely by the saturation pressures of cadmium and sulfur, respectively. The total pressure $P = p_{S_2} + p_{Cd}$ around a crystal tends towards a minimum when the crystal evaporates freely. For this minimum total pressure situation, $p_{Cd} = 2p_{S_2} = 2/3P_{min} = (\sqrt{2}K_{CdS})^{2/3}$, where K_{CdS} is the value of the evaporation constant at that temperature. If there are cooler regions in the enclosed volume where p_{Cd} or p_{S_2} is much smaller than its value corresponding to this situation, while the total pressure $(p_{Cd} + p_{S_2})$ is also low, the crystal will sublime to these regions at a rate that is greater, the higher the crystal temperature. In diffusion experiments, this pressure range has to be avoided. As a result, there are two categories of diffusion experiments:

(i) Cd* diffusion under $p_{Cd} > 2/3P_{min}$, and S* diffusion under $p_{S_2} > 1/3P_{min}$ (i.e., $p_{Cd} < 2/3P_{min}$);

(ii) Cd* diffusion under $p_{Cd} < 2/3P_{min}$ and S* diffusion under $p_{S_2} < 1/3P_{min}$ (i.e., $p_{Cd} > 2/3P_{min}$).

Experiments under the first category, where the dominant component pressure is below the saturation pressure of the pure component, are carried out using a long evacuated sealed quartz glass tube in a two-temperature furnace. The crystal is maintained at a temperature T_1, while Cd or S containing the respective tracer is maintained at a lower temperature T_2. The component pressure corresponding to T_2 is calculated from the known vapor pressure data. If the component pressure equals the saturation pressure at T_1 or is greater than one atmosphere, the sample is enclosed with the corresponding element containing the tracer in a small capsule which is maintained at T_1. The pressure is calculated from the vapor pressure data or from the measured volume of the capsule and the weight of the added element, respectively.

The second category of experiments were all performed in small capsules (1–2″ long) maintained at a constant temperature. Since the tracer component, either Cd or S, is present in minute quantities compared to the overwhelming amount of the other component (S or Cd), virtually all of it combines to form CdS. If a two-zone set up were to be used for regulating the component partial pressure, the tracer-loaded CdS would form all along the inside of the tube, condensing mostly near the colder end. This would result in very small tracer concentrations in the vapor. The component pressures involved were high enough to make it possible to determine

the needed amount of the respective component by weighing. For pressures greater than 4 atmospheres, quartz ampoules with 2 mm wall thickness were used.

Enough time was given to permit tracer penetrations from 30–200μ. By penetration is meant the maximum depth at which the tracer count from a 5μ section is at least twice the background count. The time for a certain penetration thus defined and a given D* obviously depends upon the surface concentration of the tracer, which in turn depends upon the tracer activity in the vapor and the vapor pressure. Initial experiments, where surface concentration was low and the penetrations were <20μ, resulted in erratic and erroneous p_{Cd}-independent Cd diffusivities. Later, with larger surface tracer concentrations (10^5 counts per 10 minutes) and greater penetrations, reproducible pressure dependent results were obtained. Tracer diffused in from the sides was removed by grinding ±0.5 mm of the edges of the specimen plates. Then the crystal was mounted in a jig which allowed the removal of 2 to 5μ thick sections parallel to one of the large faces by rubbing the crystal over fine grinding paper. The tracer activity in the removed section was counted in an appropriate radiation counter. Corrections were made for the background count and activity per mg of the removed material was calculated. This normalized activity is assigned to a depth x, this being the x coordinate of the center of the removed section, measured relative to the original surface. The logarithm of the normalized activity is plotted against x^2 to give the experimental penetration profile. In a few cases we used the chemical sectioning technique described by Woodbury (*17*). Although this method gave results similar to those found with the grinding method, we dropped it because of its inadaptability to S* diffusion and because of complications arising from extensive etch pit formation.

The penetration profile obtained is fitted to one of a set of theoretical profiles fitting solution (4) which are obtained with the aid of a digital computer. Each curve is for a certain Dt product. Experimental data points for a typical ^{35}S diffusion run and a theoretical curve fitting these points are shown in Fig. 3. Over 90% of the experiments gave results closely fitting one of the theoretical curves. Sometimes, the last one or two points at the tail would deviate from the theoretical curve. These were regarded as being due to dislocation diffusion and were not analyzed further. D^* is calculated from the $D^* t$ product characterizing the theoretical curve giving the best fit, using the known diffusion time t.

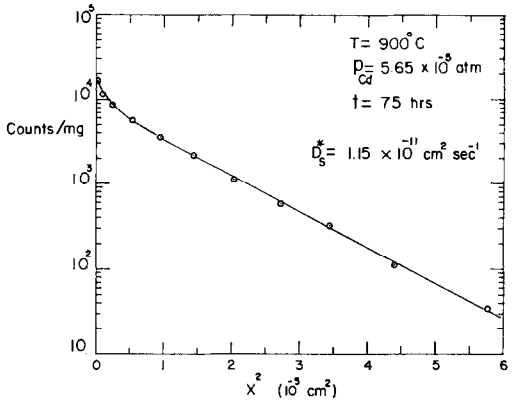

FIG. 3. Penetration profile of a typical tracer diffusion run. The curve represents a theoretical complementary error function; the points indicate experimental data for the diffusion of sulfur tracer at 900°C and $p_{Cd} = 5.65 \times 10^{-5}$ atm.

The time required for establishing the equilibrium concentrations of defects in the specimen involving chemical diffusion is negligibly small compared to the diffusion anneal time for most of the tracer diffusion experiments performed in this work. Chemical equilibration is also diffusion controlled, but is much faster than the tracer diffusion, because it depends on the microscopic diffusivities of the defects and not on the product of these constants with the defect concentration, as is the case for tracer diffusion. Experiments performed at 800°C, with and without previous equilibration under the diffusion conditions in the absence of the tracer, showed essentially no difference in the diffusion profiles. Direct confirmation of the expected much faster diffusion causing chemical equilibration was obtained from relaxation experiments. Typical times for chemical equilibration of 1 mm thick samples at 800°C were found to be 5–10 minutes. Under similar conditions of p_{Cd} and T, tracer diffusion anneal times are 3–4 days, at the end of which time the tracer distribution in the sample is still far from homogeneous, the tracer concentrations being of the order of $10^{-4} \times$ surface concentration at a depth that equals about one-tenth of the sample thickness.

However, if the absolute time for chemical equilibration becomes very long, the sample should be equilibrated prior to the tracer diffusion anneal, since tracer transport along dislocations (and other faults) during the required longer anneal time can now be appreciable and may give erratic results. Prior equilibration should also be carried out for experiments where the extra Cd or S coming out of the crystal as a result of nonstoichiometry from a previous treatment could appreciably change the

component pressure around the crystal. Keeping these considerations in mind, prior equilibration was done for experiments at low temperatures (<600°C) and at pressures corresponding to or close to the minimum total pressure; as received or doped material was used for all other experiments.

Establishment of Cd and S_2 Pressures

p_{Cd} and p_{S_2} are related by $K_{CdS} = p_{Cd}p_{S_2}^{1/2}$. As a result, low Cd-pressures can be established by establishing high p_{S_2} pressures. Since sulfur vapor contains many species other than S_2, it is necessary to see how far p_{S_2} differs from $(p_S)_{total}$. Using the results published by Shiozawa et al. (*28*), it was found that in almost all cases the conditions in our experiments were such that p_{S_2} is approximately equal to $(p_S)_{total}$.

Results and Discussion

1. Tracer Diffusion in Undoped Crystals at High Cd Pressures

The first experiments that were carried out were performed to identify the native double donor defect observed in CdS under Cd pressures from approximately 0.01 atm to saturation pressure in the temperature range 700°–1000°C (*11*), i.e., distinguish between $Cd_i^{\cdot\cdot}$ and $V_S^{\cdot\cdot}$ as the major doubly ionized native donor. Up until now (*4, 7, 9, 32*), Cd_i was considered to be the double donor without paying much attention to the chalcogen vacancy as the possible major defect. A comparison of the Cd pressure dependence of the tracer diffusivities of Cd* and S*, on the one hand, and that of the electronic conductivity and the Hall-effect (determined by the major defect), on the other, may possibly lead to the identification of the majority and minority defects. The tracer diffusivities of Cd and S were measured over the pressure range where $[e']$ measured on samples cut from the same crystal (*11*) had been found to be $\propto p_{Cd}^{1/3}$.

Results on Cd tracer diffusion in pure crystals are shown in Figs. 4 and 6. Figure 4 shows the 800° and 900°C isotherms for D_{Cd}^* as a function of p_{Cd}. In both cases, $D_{Cd}^* \propto p_{Cd}^{2/3}$. A pressure dependence of D_{Cd}^* was reported earlier by Woodbury (*17*) and Whelan and Shaw (*18*). Woodbury's results will be discussed at the end of this section. Whelan and Shaw report $D_{Cd} \propto p_{Cd}$. Their experimental points are included in Fig. 4. It is seen that the absolute values of D_{Cd}^* are in good agreement with ours whereas, as far as the slope is concerned, the points fit a line with slope

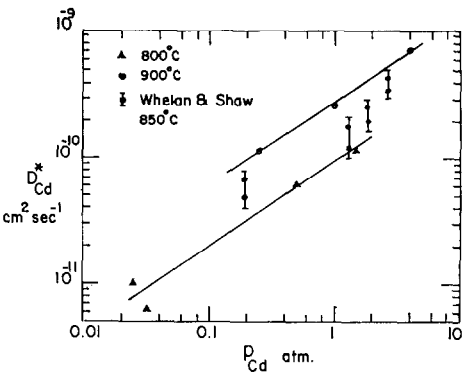

FIG. 4. Variation of D_{Cd}^* with p_{Cd} for pure CdS at 800° and 900°C; 850°C data by Whelan and Shaw (18) are also given.

2/3 almost as well as the one with slope 1 which they prefer, and which they explain by assuming that Cd tracer diffusion is controlled by neutral Cd interstitials, Cd_i^x. The latter assignment cannot be correct. As we shall see, the Cd tracer diffusion in this range is decreased by doping with donors, and such a decrease is not to be expected if the diffusing defect were neutral.

The absolute values of D_{Cd}^* reported by Woodbury (17) are 10–100 times larger than ours. This difference is probably related to the fact that Woodbury's penetration profiles seldom correspond to a single complementary error function. The profiles are either curved or consist of two error functions. In the analysis, the greatest weight is given to the points in the tail of the profile. Comparison of Woodbury's data for D_{Se}^* in CdSe (15) (a case in which he gives two D's) with our results for D_S* in CdS shows close agreement for Woodbury's smallest data. This indicates that the small-penetration data give the true bulk diffusion coefficient, the tail being probably due to a mechanism involving dislocations. The difference cannot be due to the difference in the sectioning technique. Experiments carried out by us with the chemical sectioning method used by Woodbury gave results close to those obtained using the grinding technique.

With $D_{Cd}^* \propto p_{Cd}^{2/3}$ as found by us, the defect responsible for Cd tracer diffusion cannot be the majority defect controlling charge neutrality, since $[e'] \propto p_{Cd}^{1/3}$ (*11*). This leaves us with $V_S^{\cdot\cdot}$ as the major doubly ionized donor species. To test this, S tracer diffusion was studied as a function of p_{Cd}. Figure 5 shows the 900°C isotherms of D_S^* and $[e']$ as a function of p_{Cd}. Both have a slope of 1/3. This is consistent with the neutrality condition $[e'] = 2[V_S^{\cdot\cdot}]$, $V_S^{\cdot\cdot}$ being the major doubly ionized native donor. The dependence $D_{Cd}^* \propto p_{Cd}^{2/3}$ follows from this

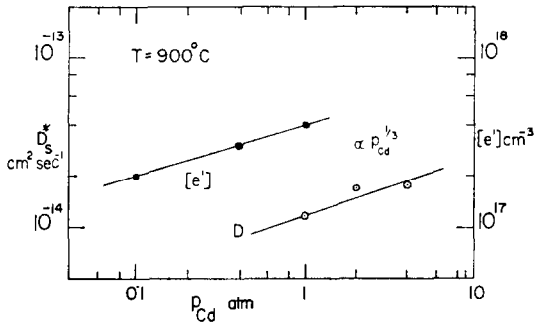

FIG. 5. Variation of D_S^* and $[e']$ with p_{Cd} at 900°C.

if Cd tracer diffusion takes place by singly ionized Cd interstitials:

$$[Cd_i^{\cdot}] = K'_{Cd_i}(2K''_{SV})^{-2/3} p_{Cd}^{2/3}. \quad (5)$$

Thus the following points are established for CdS above 700°C:

(i) The major doubly ionized native donor is $V_S^{\cdot\cdot}$.
(ii) S tracer diffusion in this p_{Cd} range is controlled by the $V_S^{\cdot\cdot}$ mechanism.
(iii) Cd_i are minority donors, and they are singly ionized.
(iv) Cd tracer diffusion is controlled by $Cd_i^{\cdot}$; as we shall see, this will be confirmed both qualitatively and quantitatively through the suppression of D_{Cd}^* by a predictable factor with heavy donor doping.

Comparing the relative magnitudes of D_{Cd}^* and D_S^* which differ by a factor of $\approx 10^4$, and realizing that $[Cd_i^{\cdot}] < [V_S^{\cdot\cdot}]$, it is clear that $Cd_i^{\cdot}$ is by far the fastest moving point defect under these conditions and should be the one involved in bringing about changes in stoichiometry in response to a changed p_{Cd} and/or T (chemical diffusion).

By virtue of the neutrality condition, $[V_S^{\cdot\cdot}]$ can be determined via Hall-effect measurements of $[e']$, and the mobility of $V_S^{\cdot\cdot}$ can then be determined from the variation of D_S^* and $[e']$ as a function of temperature.

$$[V_S^{\cdot\cdot}] = 1/2[e'] = \left(\frac{K''_{SV}}{4}\right)^{1/3} p_{Cd}^{1/3}. \quad (6)$$

From Hall-effect measurements on samples from the same crystal (*11*),

$$K''_{SV} = 1.14 \times 10^{-7} \exp(-1.75\,\text{eV/kT})\,\text{atm}^{-1}. \quad (7)$$

Therefore,

$$[V_S^{\cdot\cdot}] = 3.06 \times 10^{-3} \exp(-0.58\,\text{eV/kT}) p_{Cd}^{1/3}, \quad (8)$$

and for $p_{Cd} = 4$ atm,

$$[V_S^{\cdot\cdot}] = 4.86 \times 10^{-3} \exp(-0.58\,\text{eV/kT}). \quad (9)$$

Also at $p_{Cd} = 4$ atm, the only two successful measurements made of D_S^* as a function of temperature (at 900° and 1000°C) can be expressed as

$$D_S^* = 2.58 \times 10^{-6} \exp(-1.9\,\text{eV/kT})\,\text{cm}^2\,\text{sec}^{-1}. \quad (10)$$

Since $D_S^* = D_{V_S^{\cdot\cdot}}[V_S^{\cdot\cdot}]$, (9) and (10) lead to

$$D_{V_S^{\cdot\cdot}} = 5.32 \times 10^{-4} \exp(-1.32\,\text{eV/kT})\,\text{cm}^2\,\text{sec}^{-1}. \quad (11)$$

From the temperature dependence of D_{Cd}^* for $p_{Cd} = 1$ atm, shown in Fig. 6, we arrive at the following general expression for D_{Cd}^* valid at high p_{Cd}:

$$D_{Cd}^* = 7.29 \times 10^{-5} \exp(-1.26\,\text{eV/kT}) p_{Cd}^{2/3}\,\text{cm}^2\,\text{sec}^{-1}. \quad (12)$$

Cd_i being the minority species, their absolute concentration and hence their mobility cannot be determined. Woodbury (*17*) gives for D_{Cd}^* under saturated Cd vapor:

$$D_{Cd}^* = 3 \exp(-2.0\,\text{eV/kT})\,\text{cm}^2\,\text{sec}^{-1}.$$

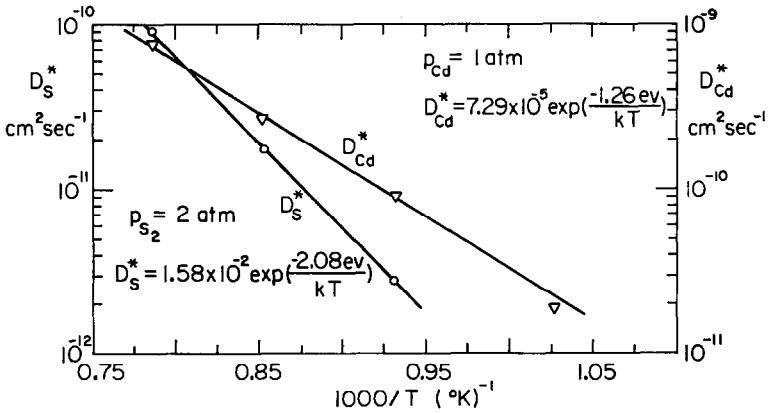

FIG. 6. Temperature variation of D_{Cd}^* at high p_{Cd} and D_S^* at high p_{S_2}(=low p_{Cd}).

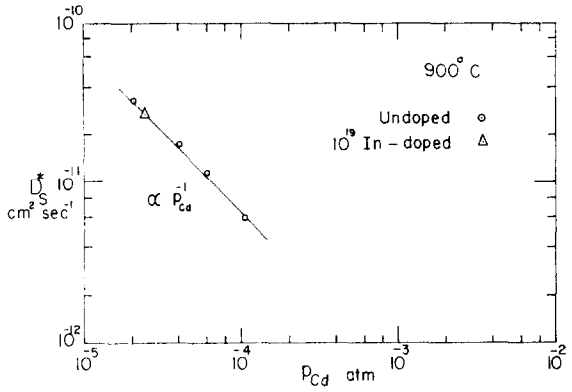

FIG. 7. D_S^* as $f(p_{Cd})$ for pure and indium doped crystals at 900°C.

Assuming a $p_{Cd}^{2/3}$ dependence, and using the cadmium saturation pressure as $f(T)$ as given by Shiozawa et al. (*28*), this leads to

$$D_{Cd}^* = 1.45 \times 10^{-3} \exp(-1.32\,\text{eV/kT}) p_{Cd}^{2/3} \quad (13)$$

not too different from (12).

2. Tracer Diffusion in Undoped Crystals at Low Cd Pressures

When passing from high p_{Cd} to low p_{Cd} (high p_{S_2}), it was found that a change in the diffusion mechanism occurs for both Cd- and S-tracer diffusion. Data on S* diffusion at low p_{Cd} are shown in Figs. 6 and 7. Figure 7 shows the 900°C isotherm for D_S^* as a function of p_{Cd}. It obeys the law $D_S^* \propto p_{Cd}^{-1}$, and strongly suggests the neutral sulfur interstitial ($S_i^\times$) as the dominant defect responsible for S-exchange. The neutral character was confirmed by comparing D_S^* measured with undoped crystals and with an indium doped sample. Indium acts as a donor in CdS, and S_i must be expected to act as an acceptor. If ionized it would form S_i' or S_i''. The concentrations of these species should increase markedly with donor doping, causing a corresponding increase in their respective contributions to the total D_S^* which would be noticeable if their concentration mobility product would be > that for $S_i^\times$. As shown in Fig. 7, no change in D_S^* was observed by doping with 10^{19} In cm^{-3}. Thus $S_i^\times$ must be and remain the species with the largest concentration-mobility product responsible for sulfur tracer exchange. Diffusion by neutral chalcogen interstitials as concluded from the inverse proportionality of D^* with the metal pressure has also been observed for Se and Te diffusion in a variety of other Cd and Zn chalcogenides (*15*, *16*) and for S*-diffusion in PbS (*14*). Independence upon doping with donors was reported only in the latter case.

The temperature dependence of interstitial D_S^* for $p_{S_2} = 2$ atm is shown in Fig. 6. The data can be represented by

$$D_S^* = 1.11 \times 10^{-2} p_{S_2}^{1/2} \exp(-2.08\,\text{eV/kT})\,\text{cm}^2\,\text{sec}^{-1}. \quad (14)$$

Since $p_{S_2}^{1/2} = K_{CdS} p_{Cd}^{-1}$, this is equivalent to a dependence $\propto p_{Cd}^{-1}$. The activation energy in (14) represents the enthalpy of migration of $S_i^\times$ plus the enthalpy of formation of $S_i^\times$ from a vapor containing S_2. Since the concentration of $S_i^\times$ is not changed by doping, the two contributions cannot be separated.

Data on D_{Cd}^* in nominally pure CdS at low p_{Cd} showed considerable scatter. However, the observed values ($\approx 10^{-11}$ cm^2 sec^{-1}) were much higher than the values of $\approx 10^{-13}$ cm^2 sec^{-1} for D_{Cd}^* by Cd_i diffusion, obtained by extrapolation from high p_{Cd}. Due to relatively long annealing times and the danger of sublimation at high temperatures, only a narrow pressure range, with p_{Cd} well below the minimum total pressure value, could be investigated. No particular pattern was deducible as far as the dependence on p_{Cd} is concerned. The scatter may be due to varying amounts of donor or acceptor impurities, which could enter the sample from the walls of the container during the experiment and could alter the native defect concentration through charge compensation. An increase in D_{Cd}^* with donor doping in this pressure range has already been reported by Woodbury (*17*). Therefore, scatter may be prevented by doing experiments with crystals, doped heavily with donors.

3. Cadmium Tracer Diffusion Experiments on Donor Doped Crystals

Practically all data on doped crystals were obtained on indium doped crystals. Figure 8 shows

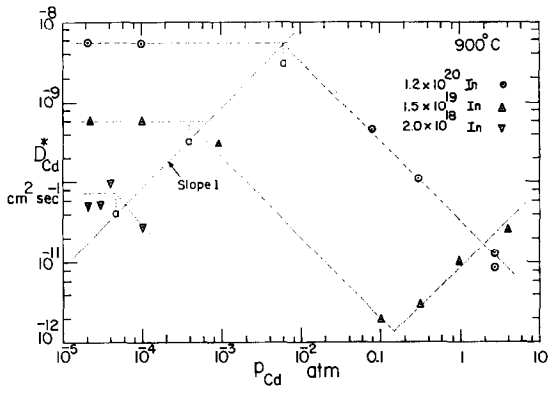

FIG. 8. Isotherms of D_{Cd}^* as $f(p_{Cd})$ for crystals doped with various concentrations of indium. The points *a* indicate $(p_{Cd})_{tr}$.

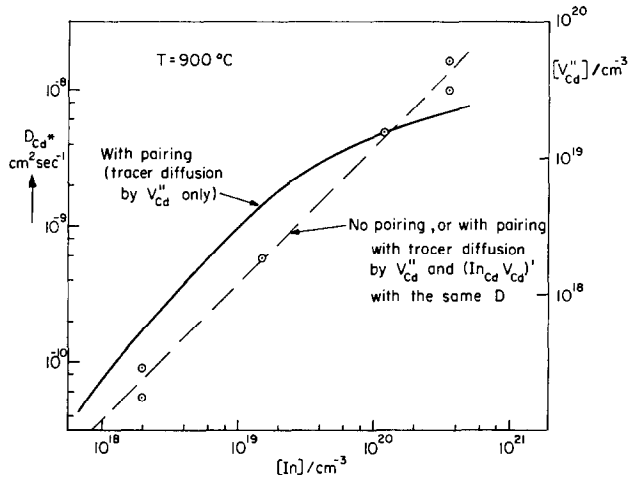

FIG. 9. The dependence of D^*_{Cd} on the indium concentration at 900°C, $p_{Cd} = 2 \times 10^{-5}$ atm ($p_{S_2} = 8$ atm).

isotherms for D^*_{Cd} as a function of p_{Cd} for three different indium concentrations. The result indicates the presence of three ranges in which D^*_{Cd} behaves differently. At low p_{Cd}, D^*_{Cd} is independent of p_{Cd}. At medium p_{Cd}, D^*_{Cd} decreases proportional to p_{Cd}^{-1}. At high p_{Cd}, D^*_{Cd} increases $\propto p_{Cd}$. Figure 9 shows the dependence of D^*_{Cd} on the indium concentration in the range where the diffusion coefficient is independent of p_{Cd}. Figure 10, finally, shows the temperature dependence of D^*_{Cd} for two different doping concentrations at Cd pressures chosen to remain inside the range where D^*_{Cd} is independent of p_{Cd}.

In interpreting these data we must try to find a model that represents the observed variations as well as possible. The general behavior of the isotherms of Fig. 8 indicate that different species are dominant in Cd* diffusion at high p_{Cd}, on the one hand, and at medium and low p_{Cd} on the other. It has already been established that the high-p_{Cd} species is $Cd_i^{\cdot}$. This is further supported by the observed dependence $\propto p_{Cd}$, to be expected for $Cd_i^{\cdot}$ when the neutrality condition is governed by $[In_{Cd}^{\cdot}] = [e']$, and the decrease in the absolute value $\propto$ [In]:

$$[Cd_i^{\cdot}]_{In} = K'_{Cd}[In_{Cd}^{\cdot}]^{-1} p_{Cd},$$

$$[Cd_i^{\cdot}]_{pure} = K'_{Cd}(2K''_{SV})^{-1/3} p_{Cd}^{2/3}$$

leading to

$$\frac{(D^*_{Cd})_{In}}{(D^*_{Cd})_{pure}} = (2K''_{SV})^{1/3} [In_{Cd}^{\cdot}]^{-1} p_{Cd}^{1/3}. \qquad (15)$$

In view of the increase of D^*_{Cd} with [In] shown in Fig. 9, the low p_{Cd} species must be a charged species, V'_{Cd}, V''_{Cd}, or $(In_{Cd} V_{Cd})'$. In either case, the species involved may, but need not be, the major charged species governing the neutrality condition; $S_i^{\times}$ found to be responsible for S* diffusion at low p_{Cd} must also be expected to be a double acceptor. A double acceptor A'' with a level close to the conduction band formed by electron bombardment and found in photoconductivity experiments (*30*) may also be

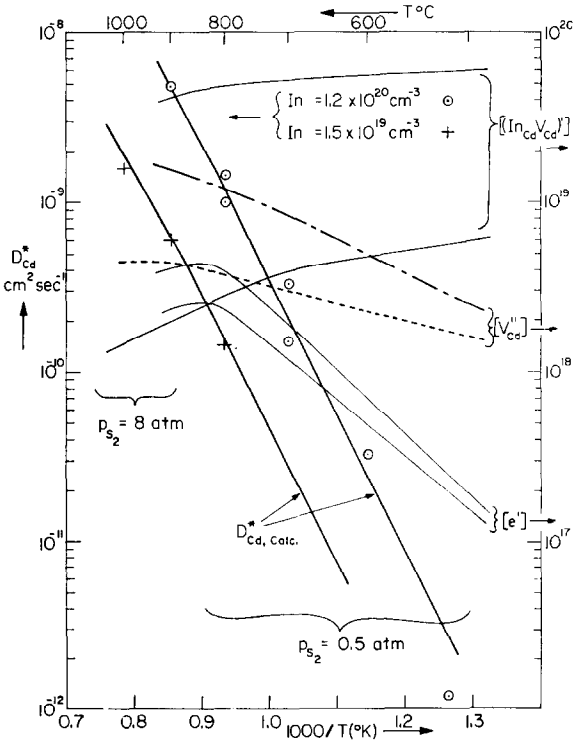

FIG. 10. Temperature dependence of D^*_{Cd} for crystals doped with 1.5×10^{19} and 1.2×10^{20} cm^{-3} indium and various p_{S_2}, calculated concentrations of V''_{Cd}, $(In_{Cd} V_{Cd})'$ and e', and D^*_{Cd} calculated using this and the mobilities listed in Table III.

either V_{Cd} or S_i (*31*). Support for cadmium vacancies rather than sulfur interstitials as the major charged native defects is found in the fact that pure In_2S_3 crystallizes in a blende type structure with the sulfur in a close-packed arrangement, and the two indium atoms distributed over three equivalent sites. On this basis we shall assume $[V'_{Cd}]$, $[V''_{Cd}] > [S'_i]$, $[S''_i]$. We are then still left with the choice between V'_{Cd}, V''_{Cd} and the associate $(In_{Cd}\,V_{Cd})'$ as the major charge compensating defect, with the approximate neutrality conditions,

$$[In^{\cdot}_{Cd}] \approx [V'_{Cd}], \tag{16}$$

$$[In^{\cdot}_{Cd}] \approx 2[V''_{Cd}], \tag{17}$$

$$[In^{\cdot}_{Cd}] \approx [(In_{Cd}\,V_{Cd})'] = \tfrac{1}{2}[In]_{total}. \tag{18}$$

The isotherms shown in Fig. 1 correspond to (17). Similar isotherms can be constructed for the other cases. All predict a transition from an essentially p_{Cd}-independent D^*_{Cd} range at low p_{Cd} to a range at medium p_{Cd} where $D^*_{Cd} \propto [V''_{Cd}] \propto p_{Cd}^{-1}$, the transition taking place at $(p_{Cd})_{tr}$. A choice between the three possibilities can be made on the basis of the variation of $(p_{Cd})_{tr}$ with the indium concentration. It is easily seen that $(p_{Cd})_{tr}$ is independent of $[In]_{tot}$ for (16), $\propto [In]_{tot}$ for (17), and $\propto [In]^2_{tot}$ for (18). The data of Fig. 8 show a variation intermediate between [In] and $[In]^2$ though close to the former. This rules out V'_{Cd} as the major species in the range next to that governed by $[In^{\cdot}_{Cd}] = [e']$, but leaves as possibilities (17) or a mixed regime with V''_{Cd} and $(In_{Cd}\,V_{Cd})'$ jointly governing the neutrality condition.

A considerable degree of pairing at concentrations $\geqslant 10^{19}$ cm^3 and temperatures as high as 900°C is indicated by results by Hershman et al. (*32*) in the high-temperature Hall effect of indium doped CdS in cadmium and sulfur vapor.

If pairs are not to be neglected, the data have to be discussed on the basis of the more complete neutrality condition

$$[In^{\cdot}_{Cd}] = [(In_{Cd}\,V_{Cd})'] + 2[V''_{Cd}] + [e'], \tag{19}$$

which, combined with the indium balance, leads to

$$[In]_{tot} = 2[(In_{Cd}\,V_{Cd})'] + 2[V''_{Cd}] + [e']. \tag{20}$$

Combination with the pairing reaction (Table I (q)) and the formation reaction for V''_{Cd} (Table I (e)) leads to the relation

$$[In]_{total} = 2K_P\,K''_{CdV}[In]_{total}\,a_e^2\,p_{Cd}^{-1}/ (1 + K_P\,K''_{CdV}\,a_e^2\,p_{Cd}^{-1}) + 2a_e^2\,K''_{CdV}\,p_{Cd}^{-1} + [e'] \tag{21}$$

in which the three terms at the right hand side correspond to the three terms in (20). $a_e = \gamma[e']$ represents the activity of the electrons, γ being the activity constant; γ becomes larger than one for electron concentrations approaching the density of states in the conduction band. For an effective mass $m_e^* \approx 0.2$ m, these densities vary from 1.74×10^{19} cm^{-3} at 900°C to 9.4×10^{18} cm^{-3} at 500°C. Values of γ may be taken from Rosenberg (*33*). Using the K_P and K''_{CdV} as found by Hershman et al. (*32*), Equation (21) can be solved for $[e']$ as

$$f(p_{Cd}, [In]_{total}, T)$$

and then yields directly $[V''_{Cd}]$ and $[(In_{Cd}\,V_{Cd})']$.

D^*_{Cd} is now to be represented by

$$D^*_{Cd} = D_{V''_{Cd}}[V''_{Cd}] + D_{InV'}[(In_{Cd}\,V_{Cd})']. \tag{22}$$

Figure 9 shows the variation of D^*_{Cd} with [In] at 900°C to be expected if

(a) pairing occurs, but $D_{V''_{Cd}} \gg D_{InV'}$, i.e., only the free vacancies transport Cd*,
(b) pairing occurs, but $D_{V''_{Cd}} \approx D_{InV'}$,
(c) no pairing occurs.

Both (b) and (c) give the observed proportionality between D^*_{Cd} and $[In]_{total}$, provided $[e'] \ll [In]$ (see (20)). As seen in Fig. 10 this condition is satisfied for the conditions applying to Fig. 9. On the other hand, (a) gives a nonlinear variation not in agreement with the data. The same approach can be followed in interpreting the temperature dependence of D^*_{Cd}, shown in Fig. 10, together with the calculated values of the concentrations of free and paired vacancies. The curvature of log D^*_{Cd} as a function of $1/T$ indicates that whereas $D_{V''_{Cd}} \approx D_{InV'}$ at 900°C, at lower temperatures where pairing becomes more important, $D_{InV'} < D_{V''_{Cd}}$. Good agreement between the experimental points and a calculated D^*_{Cd} is obtained for $D_{V''_{Cd}}$ and $D_{InV'}$ with a slightly different temperature dependence. The parameters are given in Table III. This table also contains parameters for the equilibrium constants of reactions formulated in Table I. As a result of the two-parameter representation, some of the constants which should have temperature dependent preexponentials are written with constant preexponentials. In this case, the effective enthalpy listed contains a contribution of the order of $k\bar{T}$ for each T in the preexponential: $T_{700-1000°C} \approx 3 \times 10^3 \exp(-0.1\ \text{eV/kT})$.

The estimate for $E_{V_1} + E_{V_2}$ given in Table III is based on the comparison of $H_S^{\times}$ and H''_S. The sum of the distances of the two V_{Cd} acceptor levels from the valence band is

$$E_{a_1} + E_{a_2} = 2E_{gap} - E_{V_1} + E_{V_2} = 3.94 - (<1.7) = >2.24\ \text{eV}.$$

Evidently, the acceptor levels are much farther from the valence band than the V_S donor levels are from the conduction band ($\approx$0.2 eV), an asymmetry noted before. Marked asymmetry is also indicated by the

TABLE III

VALUES OF THE PARAMETERS IN THE TWO-PARAMETER EXPRESSIONS FOR THE EQUILIBRIUM CONSTANTS OR DIFFUSION COEFFICIENTS $K = K^\circ \exp(-H^*/RT)$ OR $D = D^\circ \exp(-H^*/RT)$ ARRIVED AT ON THE BASIS OF A MODEL WITH PAIRING

Equilibrium constant	D° (cm^2 sec^{-1}) or K° (site, fr., atm)	H or E (eV)	Reference or relation
(a) K''_{SV}	1.14×10^{-7}	1.75	11
(b) K_{d_1}	7.11×10^{-3}	0.04 + 0.15	11
(c) K_{d_2}	1.8×10^{-3}	0.14 + 0.15	11
(d) K_{SV}	8.9×10^{-3}	1.27	$K''_{SV}/K_{d_1}K_{d_2}$
(e) K''_{CdV}	3.6×10^{9}	2.34	32
(f) $K_{V_1}K_{V_2}$	1.28×10^{-5}	<1.7	$K_S^\times$, K''_S
(g) K_{CdV}	4.6×10^{4}	<4	$K''_{CdV}K_{V_1}K_{V_2}$
(h) K_{SVG}	1.78×10^{11}	6.86	$K_{SV}K_{Cd,S}$
(j) K_i	0.225	2.86	$(p_{Cd})_{tr}K''_{SV}/2[In]_{total}$
(k) K''_S [a]	4.1×10^{2}	4.09	$K''_{CdV}K''_{SV}$
(l) $K_S^\times$	4.1×10^{2}	<5.6	$<H_{Cd,S}$; $K''_S K_{V_1}K_{V_2}K_{d_1}K_{d_2}$
(m) K_{CdS}	2×10^{10} atm$^{3/2}$	3.4	28
(n) $K_{Cd,S}$	2×10^{13} atm^2	5.59	$K_{CdS}K_D^{1/2}$
(o) K_D	10^6 atm	4.38	28
(p) K_{Cd}	1.7×10^{5} atm	1.08	28
(q) K_P	6.7	−0.47	32
$T_{(700-1000°C)}$	3×10^{3}	0.1	
$D_{V''_{Cd}}$	4.39	1.48	$D^*_{Cd}/[V''_{Cd}]$
$D_{InV'}$	10.8	1.58	
$D_{V''_S}$	5.32×10^{-4}	1.32	$D^*_S/[V_S^{\cdot\cdot}]$
D^*_{Cd}	$7.29 \times 10^{-5}\, p_{Cd}^{2/3}$	1.26	$D_{Cd_i}[Cd_i^\cdot]$
D^*_S	$1.1 \times 10^{-2} p_{S_2}^{1/2}$	2.08	$D_{S_i^x}[S_i^x]$

[a] If S''_i rather than V''_{Cd} should be the major ionized native acceptor species, K''_S is to be replaced by $K''_{F,S}$, the constant for the Frenkel disorder of sulfur.

parameter differences for (g) and (h); neutral sulfur vacancies are more difficult to create than neutral cadmium vacancies. The reason is that the latter are considerably stabilized by formation of bonds between adjacent sulfur atoms. These bonds are destroyed, or at least weakened, upon addition of electrons. This in turn is the reason why electron addition to the neutral $V^\times_{Cd}$ involves so much energy, i.e., why the acceptor levels are so far from the valence band. The asymmetries in vacancy formation and in donor and acceptor level positions are closely related.

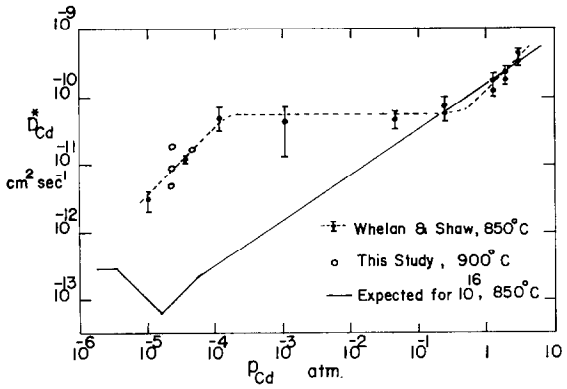

FIG. 11. D^*_{Cd} as $f(p_{Cd})$ at 850°C as reported by Whelan and Shaw (*18*), together with the variation expected for CdS with 10^{16} cm^{-3} donors on the basis of our results.

Finally, let us examine the low p_{Cd} data of Whelan and Shaw (*18*) for D^*_{Cd} at 850°C, reproduced in Fig. 11. (Their high p_{Cd} data have already been dealt with.) These authors attribute the central flat part of the isotherm as found by them to diffusion by V''_{Cd}, with $[D^*] = 2[V''_{Cd}] \approx 10^{16}$/cm^3, the neutrality condition $[D^\cdot] = 2[V''_{Cd}]$ holding over the p_{Cd} range from 10^{-4} to at least 0.15 atm. However, it is known from the Hall-effect measurements on CdS (*11*), that at 850°C, the electron concentration due to native donors is $\geqslant 10^{16}$/cm^3 for $p_{Cd} \geqslant 8 \times 10^{-5}$ atm. Thus for crystals containing 10^{16}/cm^3 foreign donors, the neutrality condition at $p_{Cd} \geqslant 10^{-4}$ atm is always $[e'] = 2[V_S^{\cdot\cdot}]$. For $p_{Cd} < 10^{-4}$ atm, the neutrality condition will be $[D^\cdot] = [e']$, both $(K''_S)^{1/2}$ and $(K_i)^{1/2}$ being less than 10^{16}/cm^3 at 850°C. The D^*_{Cd} isotherm for 10^{16} cm^{-3} donors, expected on the

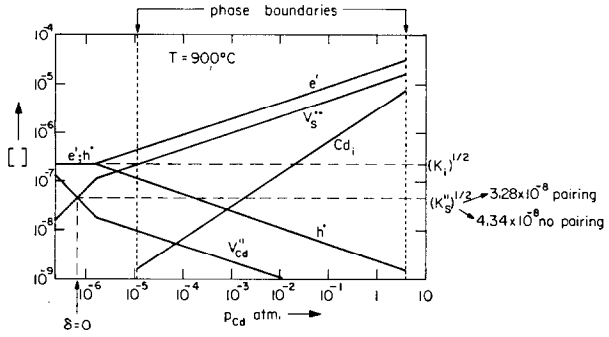

FIG. 12. Native defect concentrations at 900°C in undoped CdS, calculated for the model with pairing.

basis of our results, is shown in Fig. 11. According to these same results, a D^*_{Cd} independent of p_{Cd}, and of the magnitude as reported by Whelan *et al.* corresponds to $\approx 2 \times 10^{18}/cm^3$ donors in the crystal. But for such a donor concentration, D^*_{Cd} should remain independent of p_{Cd} down to p_{Cd}'s much smaller than shown in their results.

Whelan and Shaw attribute the dependence $D^*_{Cd} \propto p_{Cd}$ at $p_{Cd} < 10^{-4}$ atm to a corresponding variation of $[V''_{Cd}]$ to be expected when the neutrality has changed to $[D^{\cdot}] = [V'_{Cd}]$. This would imply that $(p_{Cd})_{tr} > 10^{-4}$ atm at 850°C for 10^{16} cm^{-3} and higher donor concentrations. Extrapolated values for $(p_{Cd})_{tr}$ at 850°C for 2×10^{18} cm^{-3} donors from our data are $\sim 4 \times 10^{-6}$ atm, well below 10^{-4} atm and close to the phase boundary. Thus according to our data, a range where $D^{\cdot}$ is compensated by V'_{Cd} does not fall into the stability range for $[D] = 10^{16}$ cm^{-3} and can at most be narrow at higher donor concentrations. In view of the scatter and irreproducibility noticed by us for D^*_{Cd} in undoped samples at low p_{Cd}, it is possible that their data are in error. However, the possibility of other models explaining their data cannot be excluded.

On the basis of the constants as listed in Table III, we can see how pure CdS must be expected to behave. Figure 12 shows 900°C isotherms. Figure 13 shows the position of the stoichiometric points, given by $(p_{Cd})_{\delta=0} = (K''_{CdV}/K''_{sv})^{1/2} K_i$, relative to the phase boundaries of CdS; at all T the stoichiometric composition falls outside the stability limits of the phase. In the same figure we have indicated $(p_{Cd})_{native}$ above which the concentration of electrons due to nonstoichiometry becomes larger than that from the foreign donors; we also give $(p_{Cd})_{tr}$. Figure 14 shows the expected effect of doping with acceptors at 900°C, $p_{Cd} = 2 \times 10^{-5}$ atm. Holes become the majority species at a foreign acceptor concentration of 3×10^{-6}. Considering that the electron mobility is 10–100 × the hole mobility, doping concentrations that are at least 10 times higher are required to find a p-type Hall effect or thermoelectric power.

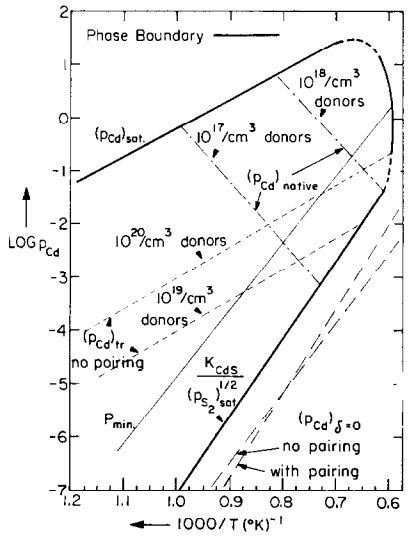

FIG. 13. Positions of the stoichiometric composition $(p_{Cd})_{\delta=0}$, and $(p_{Cd})_{tr}$ and $(p_{Cd})_{native}$ for different donor concentrations relative to the three-phase line (the s-l-g phase boundary) of CdS.

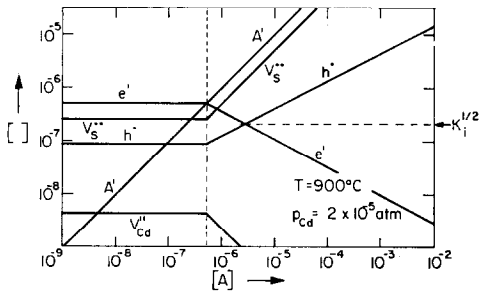

FIG. 14. Expected defect concentrations as a function of the concentration of foreign acceptors at $p_{Cd} = 2 \times 10^{-5}$ atm ($p_{S_2} = 8$ atm) and 900°C.

Conclusions

Cd and S tracer diffusivity measurements on undoped crystals show that above 700°C the diffusion data are consistent with the following:

(i) At high p_{Cd}, S diffuses via doubly ionized S vacancies, $V_S^{\cdot\cdot}$; these vacancies are also the major doubly ionized native donors reported earlier from Hall-effect measurements. Under these conditions both $[e']$ and D_S^* vary as $p_{Cd}^{1/3}$ at a constant temperature.

(ii) At high p_{Cd}, Cd diffuses as singly ionized Cd interstitials, $Cd_i^{\cdot}$; these interstitials are minority donors. Assumption of this species leads to the observed dependence $D_{Cd}^* \propto p_{Cd}^{2/3}$ at a constant temperature. $Cd_i^{\cdot}$ has a much higher mobility than $V_S^{\cdot\cdot}$, so that the concentration-mobility product is larger for $Cd_i^{\cdot}$ than for $V_S^{\cdot\cdot}$. This is indicated by the fact that $D_{Cd}^* \gg D_S^*$ under identical p_{Cd} and T.

(iii) At high S pressures (i.e., low p_{Cd}), S diffuses as neutral interstitials, $S_i^{\times}$. The neutral character follows from the observed $D_S^* \propto p_{Cd}^{-1}$ and is further established by the independence of D_S^* from donor doping.

(iv) At high S_2 pressures, Cd diffuses via doubly ionized Cd vacancies, V_{Cd}''. Even in our purest crystals, the concentration of these vacancies is controlled by foreign impurities which makes D_{Cd}^* under these conditions independent of pressure. In pure or weakly doped crystals, the mobility concentration products for Cd* and S* diffusion are of the same order.

Cd tracer diffusivity measurements on In-doped crystals above 700°C show that

(i) At high S_2 pressures and for heavily doped crystals, In is incorporated as $In_{Cd}^{\cdot}$ with the formation of doubly ionized acceptors as the charge compensating species. Pairing between $In_{Cd}^{\cdot}$ and V_{Cd}'' is important at indium concentrations $\geq 10^{19}$ cm^3 at all temperatures.

(ii) If V_{Cd}'' are assumed to be the major acceptors, interpretation of D_{Cd}^* data on the basis of a model including pairing leads to expressions for the various equilibrium constants and the microscopic mobilities of V_{Cd}'' and $(In_{Cd} V_{Cd})'$ as given in Table III.

References

1. F. A. KRÖGER AND H. J. VINK, "Solid State Physics III" (F. Seitz and D. Turnbull, Eds.), p. 307. Academic Press, New York, 1956; F. A. KRÖGER, "The Chemistry of Imperfect Crystals," North Holland, Amsterdam, 1964.
2. F. A. KRÖGER, H. J. VINK, AND J. VAN DEN BOOMGAARD, *Z. Phys. Chem.* **203**, 1 (1954).
3. K. W. BOER, R. BOYN, AND O. GOEDE, *Phys. Status Solidi* **3**, 1684 (1963).
4. R. BOYN, O. GOEDE, AND S. KUSCHNERUS, *Phys. Status Solidi* **12**, 57 (1965).
5. M. HUNG, N. OHASHI, AND K. IGAKI, *Jap. J. Appl. Phys.* **8**, 652 (1969).
6. F. T. J. SMITH, *Solid State Comm.* **8**, 263 (1970).
7. R. C. WHELAN AND D. SHAW, *Phys. Status Solidi* **29**, 145 (1968).
8. F. T. J. SMITH, *Met. Trans.* **1**, 617 (1970).
9. K. ZANIO, *J. Appl. Phys.* **41**, 1935 (1970).
10. O. A. MATVEEV, YU. V. RUD, AND K. V. SANIN, *Sov. Phys. Semicond.* **3**, 779 (1969).
11. G. H. HERSHMAN AND F. A. KRÖGER, *J. Solid State Chem.* **2**, 483 (1970).
12. C. WAGNER, *J. Chem. Phys.* **18**, 62 (1950).
13. M. S. SELTZER AND J. B. WAGNER, JR., *J. Phys. Chem. Solids* **24**, 1525 (1963).
14. M. S. SELTZER AND J. B. WAGNER, JR., *J. Phys. Chem. Solids* **26**, 233 (1965).
15. H. H. WOODBURY AND R. B. HALL, *Phys. Rev.* **157**, 641 (1967).
16. P. M. BORSENBERGER AND D. A. STEVENSON, *J. Phys. Chem. Solids* **29**, 1277 (1968).
17. H. H. WOODBURY, *Phys. Rev. A* **134**, 492 (1964).
18. R. C. WHELAN AND D. SHAW, *Phys. Status Solidi* **36**, 705 (1969).
19. P. M. BORSENBERGER, D. A. STEVENSON, AND R. A. BURMEISTER, JR., "II–VI Semiconducting Compounds," (D. G. Thomas, Ed.), p. 439. Benjamin, New York, 1967.
20. R. C. WHELAN AND D. SHAW, Ibid., p. 451.
21. J. S. PRENER AND F. E. WILLIAMS, *J. Chem. Phys.* **25**, 361 (1956); A. SCHLEEDE, *Chem. Ber.* **90**, 1162 (1957).
22. P. H. KASAI AND Y. OTOMO, *Phys. Rev. Lett.* 7, 17 (1961); *J. Chem. Phys.* **37**, 1263 (1962).
23. J. S. PRENER AND D. J. WEIL, *J. Electrochem. Soc.* **106**, 409 (1959).
24. F. A. KRÖGER, "The Chemistry of Imperfect Crystals," Ch. 16, pp. 680–684, North Holland, Amsterdam, 1964.
25. G. BROUWER, *Philips Res. Rep.* **9**, 366 (1954).
26. J. CRANK, "The Mathematics of Diffusion," p. 18, Oxford University Press, Oxford, 1957.
27. L. J. VAN DER PAUW, *Philips Tech. Rev.* **20**, 220 (1959).
28. L. R. SHIOZAWA AND J. M. JOST, *Aerospace Res. Lab. Rep.* 69-0107, Office of Aerospace Research, United States Air Force, Wright-Patterson Air Force Base, Ohio, July 1969.
29. J. C. FISHER, *J. Appl. Phys.* **22**, 74 (1951).
30. E. NEBAUER, *Phys. Status Solidi* **29**, 269 (1968); M. R. LORENZ AND H. H. WOODBURY, *Phys. Rev. Lett.* **10**, 215 (1963).
31. F. A. KRÖGER, *J. Phys. Chem. Solids* **26**, 1717 (1965).
32. G. H. HERSHMAN, V. P. ZLOMANOV, AND F. A. KRÖGER, *J. Solid State Chem.* **3**, 401 (1971).
33. A. J. ROSENBERG, *J. Chem. Phys.* **33**, 665 (1960); Ref. (**24**, pp. 212–214).
34. W. D. CALLISTER, JR., C. F. VAROTTO, AND D. A. STEVENSON, *Phys. Status Solidi* **38**, K 45 (1970).